Experimental report

09/01/2026

Proposal: 9-13-1084 **Council:** 4/2023

Title: Nanostructural investigation on how different lipids and glycosylation can affect protein-lipid interactions.

Research area: Biology

This proposal is a new proposal

Main proposer: Beatrice BARLETTI

Experimental team: Giovanna FRAGNETO
Beatrice BARLETTI
Marco MACCARINI

Local contacts: Nicolo PARACINI

Samples: POPC solution
POPC/POPS 90:10 solution
POPC/DOTAP 70:30 solution
POPC/SM/CHOL 60:30:10 solution
POPC/SM/CHOL 50:25:25 solution
alpha-fetoprotein solution

Instrument	Requested days	Allocated days	From	To
FIGARO	3	3	03/11/2023	06/11/2023
D17	3	0		

Abstract:

We propose to draw a mechanistic understanding of the molecular mechanisms responsible for protein/lipid interactions by performing nanostructural characterisation with neutron reflectometry. This proposal is an integral part of an INNOVAXN PhD grant, which was awarded in 2021 to Mme Beatrice Barletti for the development of a smart biomedical biosensor based on nanostructured biomimetic lipid membranes. The results from this experiment will provide essential structural information for the interpretation of our initial functional investigations that demonstrated the interaction of glycosylated and non-glycosylated protein biomarkers with biologically relevant lipid bilayer membranes. The investigated protein will be alpha-fetoprotein which is a sensitive biomarker for liver cancer found in the blood.
Particularly we will identify how different lipids and glycosylation can affect this interaction. To better discriminate the effect of glycosylation, the resulting data will be compared with data from two different previously studied proteins, sVE and BSA. the comparison between their behaviours will provide a general picture of the interaction between proteins and lipidic moieties.

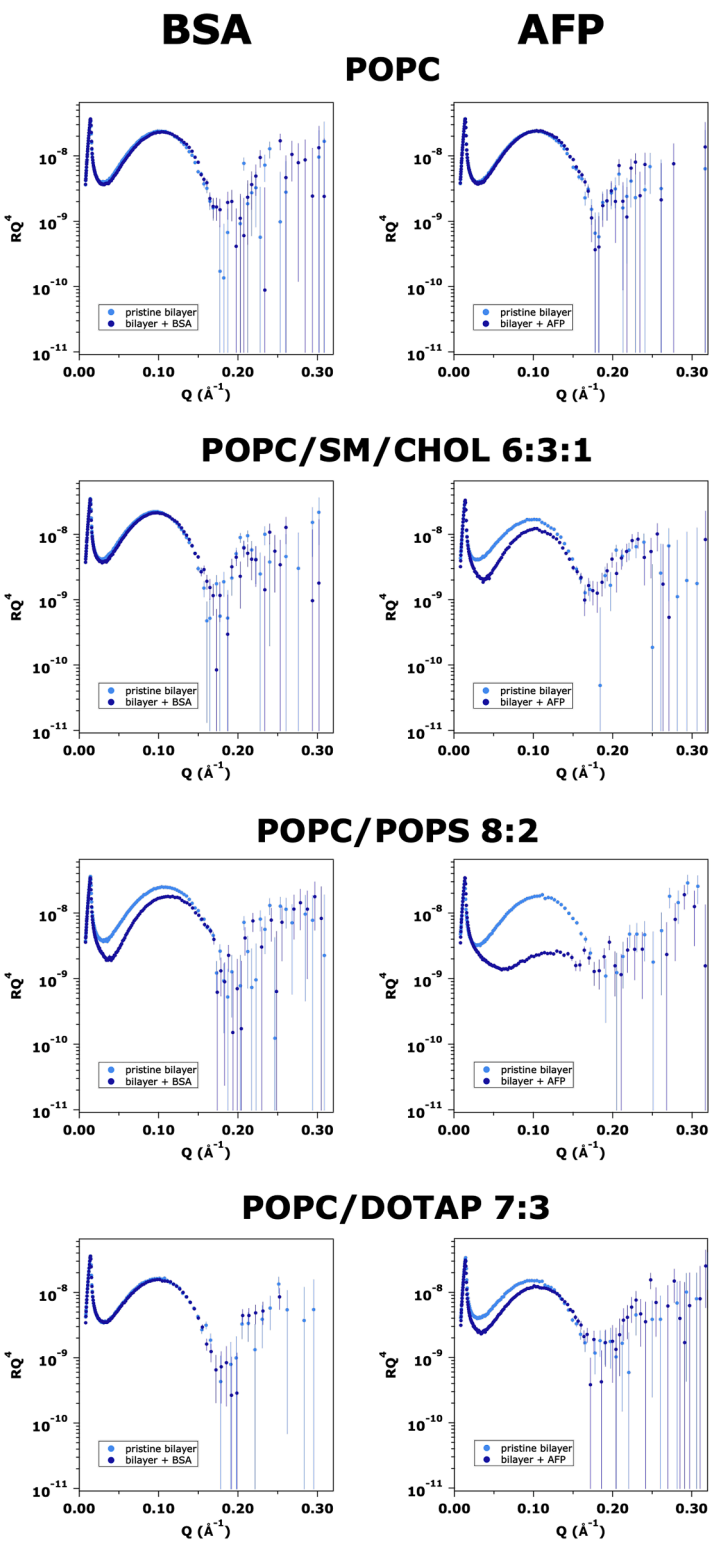

Fig. 3. Reflectivity profiles in the D_2O contrast for the four types of SLB before and after the exposure to BSA and AFP. BSA data from reference [30].

value was chosen as the one that best represented the data. Accordingly, the fitting parameters (Table 2) confirmed no relevant changes in the structural characteristics of the POPC bilayer upon AFP exposure. These results demonstrate that AFP does not significantly interact with or incorporate into POPC membranes under the conditions tested.

5.2.2. POPC/SM/Chol 6:3:1

Fig. 4 displays the reflectivity profiles at different contrasts of the SLB with composition POPC/SM/CHOL 6:3:1 before and after the exposure to AFP, together with the best-fit curves, SLD and volume fraction profiles. After testing different models and evaluating both χ^2 values and posterior distributions of key parameters, the best fit was obtained

with the partial incorporation of AFP into the outer leaflet without an additional adsorbed protein layer onto the SLB (model 3b, see Figure S1 in the SI). The χ^2 value obtained for Model 3, which includes a putative extra layer representing the portion of protein protruding into the aqueous phase above the bilayer, is very close to that of Model 3b. However, analysis of the posterior distributions for this model (corner plot in Figure S9 in the Supporting Information) indicated that the supplemental layer lacks physical relevance, as its thickness distribution peaks around 0 Å. Including such a layer would therefore count as overparameterization rather than providing a meaningful description of the system.

The selected model (fitting parameters shown in Table 2) indicates that AFP was incorporated in the outer leaflet of the SLB with a volume fraction of 38%. The incorporation of the protein is accompanied by a decrease in the thickness of the inner head region and an increase in the hydration of the SLB, especially in the proximal leaflet. The penetration of AFP into the outer leaflet might induce defects and disorder in the overall structure of the SLB, exposing the bilayer to penetration of water. In the distal leaflet, the water is replaced by the protein, mitigating the amount of water present in this region. In the proximal leaflet, the increase in the solvent penetration is likely linked to the removal of lipids after the interaction with the protein and successive rinsing of the liquid phase, which are not replaced by the proteins that remain in the distal region.

While the radius of gyration (Rg) of AFP has not been experimentally determined in literature, the protein shares a comparable molecular weight and overall fold with serum albumins. Accordingly, an Rg in the same range as that reported for albumins can be reasonably assumed as a first approximation. The radius of gyration for proteins such as human and bovine serum albumin is approximately 27–29 Å[18,59]. In low-resolution experiments like neutron reflectometry, this value represents the characteristic length scale associated with the protein's spatial distribution. Given that the thickness of the outer lipid leaflet is 23 Å and that this layer is typically smoothed by a 5 Å roughness on both interfaces, the effective thickness of the outer leaflet remains compatible with the incorporation of the protein within this region.

Based on these findings, AFP interacts with zwitterionic membranes containing SM and CHOL through partial incorporation into specific regions of the bilayer. This behavior might be likely influenced by the presence of ordered nanodomains, as the inclusion of SM and CHOL markedly alters AFP binding compared to pure POPC SLBs. These observations align with previous studies demonstrating the role of ordered nanodomains in promoting protein-lipid interactions [60–62].

5.2.3. POPC/POPS 8:2

As shown in Fig. 3, the interaction of AFP with the POPC/POPS (8:2) SLB induces drastic changes in the reflectivity profile. The reflectivity profiles of the SLB before and after the exposure to the AFP together with the fitting curves of the best model, and the resulting SLD and volume fraction profiles are reported in Figure S10. While the pristine SLB was well described using the standard bilayer model, none of the bilayer-based models could adequately fit the data after AFP exposure. A representative example of a fit using a model that includes a bilayer slab structure is presented in Figure S11 (Supporting Information). This figure highlights the significant discrepancies between the experimental reflectivity profiles and those generated by the model fit.

Instead, the simplest and more accurate representation of the data was obtained with a single unstructured slab of intermediate SLD between lipid and protein (model 6), indicating that the bilayer structure was heavily disrupted. These findings suggest that AFP strongly interacts with negatively charged membranes, where electrostatic interactions drive significant bilayer destabilization and mixing of lipids with proteins on the substrate.

5.2.4. POPC/DOTAP 70:30

The reflectivity profiles of the SLB with composition POPC/DOTAP 7:3 before and after the exposure to AFP together with the fitting curves of the best model and the resulting SLD and volume fraction profiles are reported in Figure S12 in the Supporting Information. In this case, the interaction with AFP was best represented by the formation of an adsorbed protein layer of approximately 39 Å thickness and a volume fraction of around 5%, without any incorporation of the protein into the SLB (model 1, see Figure S1). The fitting parameters are listed in Table 2. The resulting thickness of the adsorbed protein layer is consistent with physical dimensions of AFP. Moreover, the interaction with the proteins induces a thickening of the tail region and an increasing of hydration of the head and tail region. This is consistent with removal of a fraction of the lipids by AFP. Based on these results, electrostatic interactions between AFP and the positively charged lipid might be the main driving force for the observed behaviour, given that at physiological pH AFP is negatively charged.

Fig. 5 provides a summary of the NR results, highlighting the interactions of BSA and AFP with the four different lipid compositions.

6. Molecular dynamics simulations of protein-membrane interactions

6.1. Protein-membrane binding and contact frequency

To assess membrane association, we first computed the fraction of bound versus unbound states, defining a protein as "bound" when any of its non-hydrogen atoms were within 10 Å of a lipid (Fig. 6A). While both proteins display similar binding propensities, the extent and nature of their interactions depend strongly on the membrane composition. In particular, BSA and AFP remained closely associated with DOTAP-containing membranes throughout most of the simulation time, suggesting that electrostatic interactions are a key driver of membrane binding captured by the MD simulations. This trend was confirmed by a detailed contact analysis (Figure S13). Both proteins formed the highest number of contacts in DOTAP-containing membranes: BSA made ~ 74 lipid contacts, and AFP made ~ 100 contacts during the final 200 ns (Fig. 6B). For the other membrane compositions, contact numbers were lower and similar across both proteins. As all systems primarily contain POPC, it accounts for the majority of contacts; however, the presence of DOTAP enhances the interaction frequency.

6.2. Lipid occupancy and interaction surfaces

To further localize protein-lipid interaction sites, we analyzed lipid occupancies per residue over the final 200 ns of the simulation (Fig. 6C-E for AFP and S14A-C for BSA). Structural domains and subdomains of BSA and AFP were visualized based on previously established classifications (ref [63]. and ref [25]., respectively). Both proteins adopt heart-shaped, asymmetric folds dominated by α-helices and loop regions, and organized into three domains (I-III), each with two subdomains (A and B).

Fig. 6D (AFP) and S14B) (BSA) show lipid occupancies per residue for the four different membrane compositions: Lipid occupancies for both proteins are broadly distributed across all three domains, with domains I and II showing the highest values. In DOTAP-containing membranes, POPC exhibits the highest occupancy, consistent with the contact frequency analysis. For clarity, values above 40% were capped in the visualizations, although some residues reached up to 51% in BSA and 77% in AFP.

Finally, surface representations of lipid-interacting residues (Fig. 6E for AFP and S14C for BSA) revealed distinct interaction patterns. BSA showed a relatively uniform binding interface across domains I and II, whereas AFP's interactions were more localized, particularly around a flexible loop region that is absent in BSA. These findings suggest that specific structural motifs contribute to differences in membrane interaction between the two proteins.

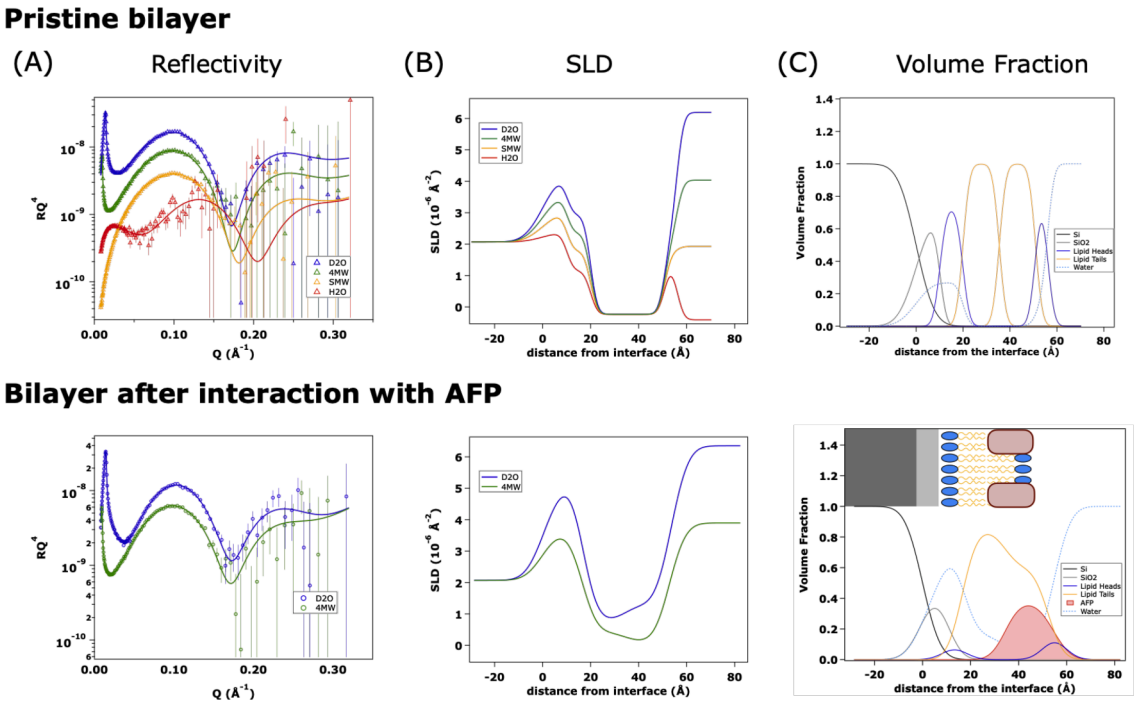

Fig. 4. Reflectivity curves and fits at different contrasts (A), the SLDs obtained from the analysis (B), and the corresponding volume fraction distribution (C) of the SLB POPC/SM/Chol 6:3:1 before and after the exposure to the AFP. Symbols represent the raw data; continuous lines represent the fit. The model that describes the experimental behavior better is the model representing a partial penetration of the protein in the outer leaflet of the lipid bilayer with no adsorbed layer of proteins onto the SLB (model 3b).

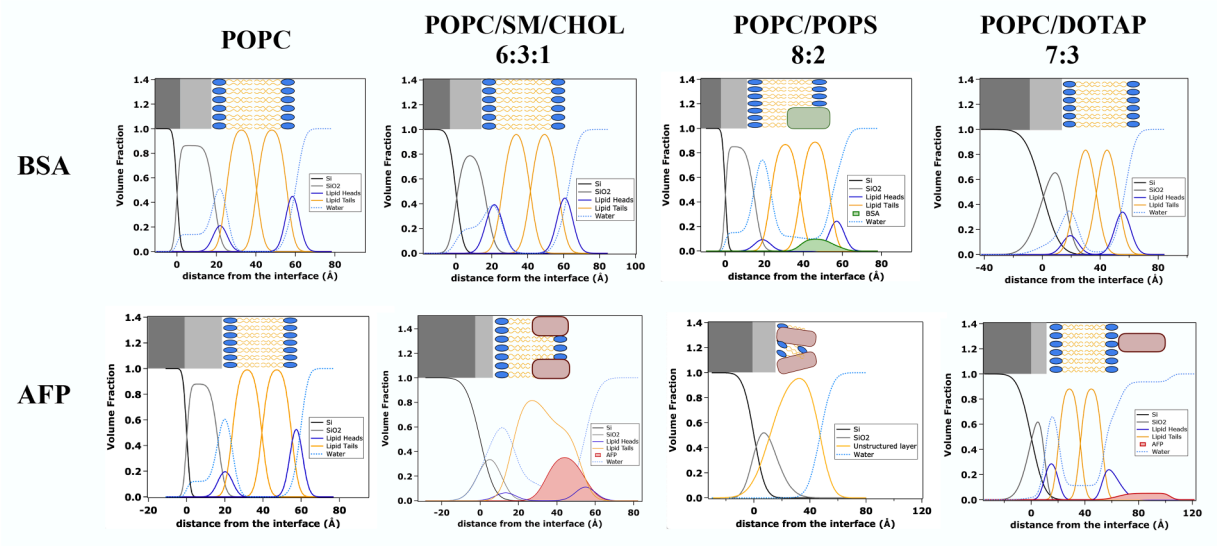

Fig. 5. Volume fraction profiles corresponding to the best-fit of the reflectivity data, illustrating how BSA and AFP interact with each of the four SLB lipid compositions. BSA data from reference [30].

6.3. Lipid depletion and enrichment near proteins

To investigate the local lipid composition around the proteins, we calculated the depletion/enrichment index (Fig. 7A), which compares the local abundance of lipids near the protein with its abundance in the bulk membrane. Surprisingly, POPS was the most enriched lipid near both proteins despite a relatively low overall contact number. In contrast, DOTAP was depleted in the vicinity of both BSA and AFP. This may seem counterintuitive given the large net negative charge of both proteins (BSA: -16e; AFP: -17e), but it reflects the presence of positively charged surface patches on the proteins that drive localized interactions (Figures S13 and S16 in the supporting information). This interpretation aligns with experimental findings that both proteins insert into POPS-containing supported bilayers. Cholesterol showed the most substantial depletion, likely due to its deep position within the membrane; almost no cholesterol molecules were detected within the 10 Åinteraction cut-off in any simulation snapshot.

6.4. Membrane thickness and domain formation

Next, we examined how lipid composition affects the membrane structure by calculating the average membrane thickness, defined as the